SPARC_LAB
Sources for Plasma Accelerators and Radiation Compton with Lasers and Beams

M. Ferrario (Resp. Naz.), D. Alesini, M. P. Anania (Ass. Ric.), F. Anelli (Art. 15), M. Bellaveglia (Art. 23), R. Boni (Ass.), L. Cacciotti (Tecn.), M. Castellano (Ass.), E. Chiadroni, P. Chimenti (Art. 15), D. Di Giovenale (Art. 23) G. Di Pirro, A. Drago, A. Gallo, C. Gatti, G. Gatti, A. Ghigo, V. Lollo (Tecn.), M. Migliorati (Ass.), A. Mostacci (Ass.), E. Pace, L. Palumbo (Ass.), L. A. Rossi (Art. 23), R. Sorchetti (Tecn.), B. Spataro, S. Strabioli, (Art. 15), C. Vaccarezza, F. Villa (Ass. Ric.).

Participant institutions: other INFN sections (Mi, RM1, RM2, Bo, Pi, Fe, Le, Fi, Na, LNS, Ba, Ca, Ts), ENEA-Frascati, CNR-INO-Pisa

1 Introduction

A new facility named SPARC_LAB (Sources for Plasma Accelerators and Radiation Compton with Lasers and Beams) has been recently launched at the INFN National Laboratories in Frascati, merging the potentialities of the former projects SPARC [1] and PLASMONX [2]. Ten years ago in fact, a robust R&D program on ultra-brilliant electron beam photoinjector and on FEL physics, the SPARC project, a collaboration among INFN, ENEA and CNR, was approved by the Italian Ministry of Research and located at the INFN National Laboratories in Frascati.

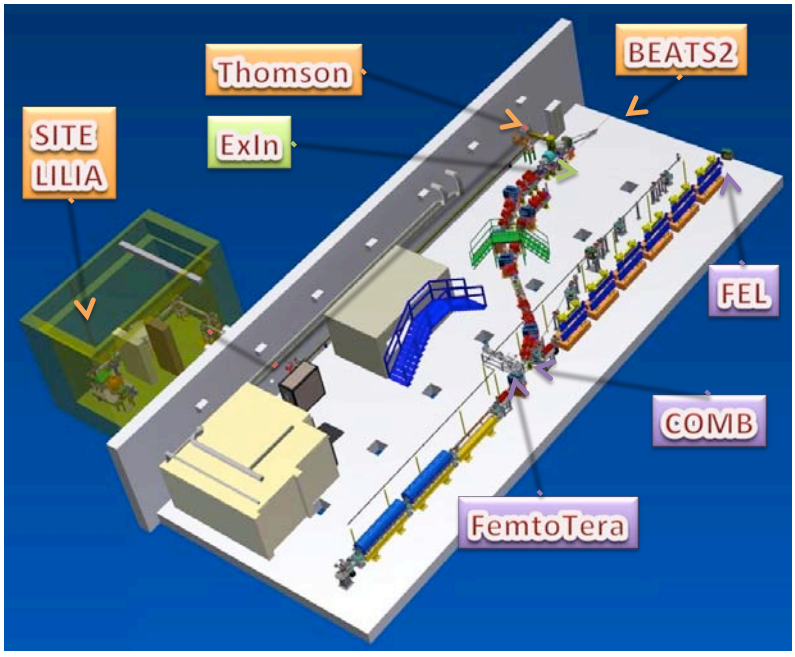

Figure 1.1: Layout of the SPARC_LAB facility with the experiments

The test facility is now operating, hosting a 150 MeV high brightness electron beam injector [3], able to operate also in the velocity bunching configuration [4], which feeds a 12 meters long undulator (*FEL experiment*). Observations of FEL radiation in the SASE [5], Seeded [6] and HHG [7] modes have been performed from 500 nm down to 40 nm wevelength. A parallel beam line is used to test new diagnostics tools, like Electro Optical Sampling. A narrow band THz radiation source [8] (*experiment TERASPARC*) is now located at exit of the linac. In parallel to that, INFN decided to host a 200 TW laser that will be linked to the linac and devoted to explore laser-matter interaction, in particular with regard to laser-plasma acceleration of protons (*experiment LILIA*) and electrons [9] in the self injection mode (*experiment SITE*) and external injection mode (*experiment EXIN*). The facility will be also used for particle driven plasma acceleration experiments [10], (*COMB experiment*). A Thomson back-scattering experiment coupling the electron bunch to the high-power laser to generate coherent monochromatic X-ray radiation is also in the commissioning phase (*experiment THOMSON*). An upgrade of the linac energy is also foreseen by the end of 2013 by installing two new high gradient C-band structures developed at LNF in the framework of the ELI_NP collaboration [18]. In Figure 1.1 the layout of the facility is shown.

The SPARC_LAB high power laser system, named FLAME, has been recently fully commissioned. FLAME is based upon a Ti:Sa, chirped pulse amplification (CPA) laser able to deliver up to 220 TW laser pulses, 25 fs long, with a 10 Hz repetition rate at a fundamental wavelength of 800 nm, see Figure 1.2.

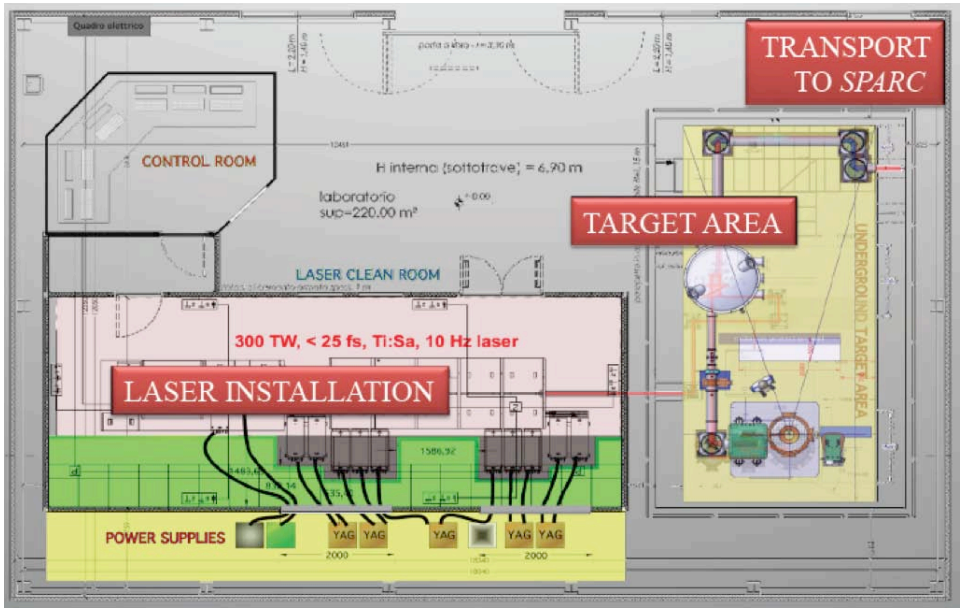

Figure 1.2: Layout of the FLAME laser with the target area for self-injection plasma acceleration experiments.

The system features a high contrast ratio (>10^{10}) and has a fully remotely controlled operation mode. It includes a front-end with pulse contrast enhancement, bandwidth control and regenerative amplifier and yields pulses with 0.7 mJ in 80 nm bandwidth. These pulses are then further amplified by the first amplifier up to 25 mJ while the second amplifier brings the energy up to the 600 mJ. The third

cryogenic amplifier is based on a 50 mm Ti:Sa crystal pumped by 10 frequency doubled Nd:YAG laser pulses, reaching an energy up to 20 J at 532 nm. The extraction energy is as high as 35%, leading to a final energy in the stretched pulses in excess of 7 J. The pulse is then compressed to a minimum pulse duration below 30 fs. Once compressed, the pulse is transported under vacuum to the target area via remotely controlled beam steering mirrors. In the typical experimental conditions of laser wakefield acceleration in self-injection configuration, the laser pulse is focused at peak intensities exceeding 10^{18} W/cm^2 which, with our ASE contrast, gives a precursor laser intensity on target below 10^9 W/cm^2. In the case of interaction with gases with pressures ranging from 1 to 10 bar, this laser intensity is below the plasma formation threshold for laser pulses of sub-nanosecond duration which is the typical duration of ASE pulses. Therefore we can reasonably assume that in the case of interaction with gases, no premature plasma formation occurs and the CPA pulse can be focused directly in the gas.

Among the different uses of FLAME, the scientific program includes self-injection and external injection [19] experiments and the realisation of an X-ray source based on the Thomson backscattering process. To this purpose, a careful characterization of FLAME performances, with particular reference to the transverse beam quality was carried out during the commissioning. The measured Strehl ratio is greater than 50% up to pulse energies of approximately 6J. For energies between 6 and 7 J, the phase front distortion increases leading to a reduction of the Strehl ratio to a minimum value of 35%. Our measurements show that the phase front pattern remains very stable from shot to shot at a given pulse energy. This makes the phase front correction with adaptive optics (planned for installation by the end of 2012) a reliable and complete solution to achieve a high quality focal spot.

We describe hereafter in more details the status and the achievements of the SPARC_LAB experiments during the year 2012.

References

[1] D. Alesini et al., Nucl. Instr. and Meth. A 507, 345 (2003).
[2] D. Giulietti et al., Proc. of PAC 2005, Knoxville, Tennessee, USA.
[3] M. Ferrario et al., Phys. Rev. Lett. 99, 234801,(2007)
[4] M. Ferrario et al., Phys. Rev. Lett. 104, 054801 (2010)
[5] L. Giannessi et al., Phys. Rev. Lett. 106, 144801 (2011).
[6] M. Labat et al., , Phys. Rev. Lett. 107, 224801 (2011).
[7] L. Giannessi et al., Phys. Rev. Lett. 108, 164801 (2012).
[8] E. Chiadroni et al., Journal of Physics: Conference Series 357 (2012) 012034.
[9] L. A. Gizzi et al., Europ. Phys. Journal - Special Topics 175, 3 (2009).
[10] M. Ferrario et al., Nucl. Inst. and Meth. A, V. 637, 1, May 2011, S43-S46
[11] P. Oliva et al., Nucl. Instrum. Meth. A 615 93-99, (2010)
[12] A. Bacci et al, Nucl. Instrum. Meth. A 608 S90-S93, (2009)
[13] U. Bottigli, et al., Il Nuovo Cimento, 29C , N.2 , 2006.
[14] A. Mostacci et al., TUPPD055, these proceedings.
[15] P. Muggli, Proc. of PAC 2009, Vancouver, Canada
[16] A. Bacci et al, Proc. of FEL Conf. 2011, Shanghai, China.
[17] P. Tomassini, private communication.
[18] C. Vaccarezza, TUOBB01, proceedings of IPAC 2012.

[19] A. R. Rossi, WEEPPB002, proceedings of IPAC 2012.

2 SITE experiment

M. P. Anania (Ass. Ric.), L. Cacciotti (Tecn.), D. Di Giovenale (Art. 23) G. Di Pirro, A. Drago, A. Gallo, C. Gatti, G. Gatti, V. Lollo (Tecn.), F. Villa (Ass. Ric.).

Participant institutions: other INFN sections (Mi, RM1, RM2, Bo, Pi,), CNR-INO-Pisa (L.A. Gizzi, Resp. Naz)

The control of ultra-high gradient laser-plasma acceleration [1] is being pursued worldwide and advanced schemes [2] are being proposed for the future staged configurations. Meanwhile, existing laser-plasma accelerating scheme are being considered for the development of all-optical radiation sources. In view of this perspective [3], experimental runs dedicated to laser-plasma acceleration experiment with self- injection (NTA_SITE) [4] have been performed at FLAME based on previous pilot experiments [5]. The first run was carried out during the early commissioning stage in 2010 at relatively low laser power (≈10 TW), and showed successful generation of mono-energetic, high energy electron bunches with a moderate to high degree of collimation down to the 6 mrad level [6]. These results were also described in the previous issues of the LNF report with an overview of the experimental set up. A second experiment at higher laser power (≈100 TW) was carried out in July 2012 and enabled us to further explore the experimental configurations [6, 7]. Here we present some preliminary highlights of the results of the observed acceleration process.

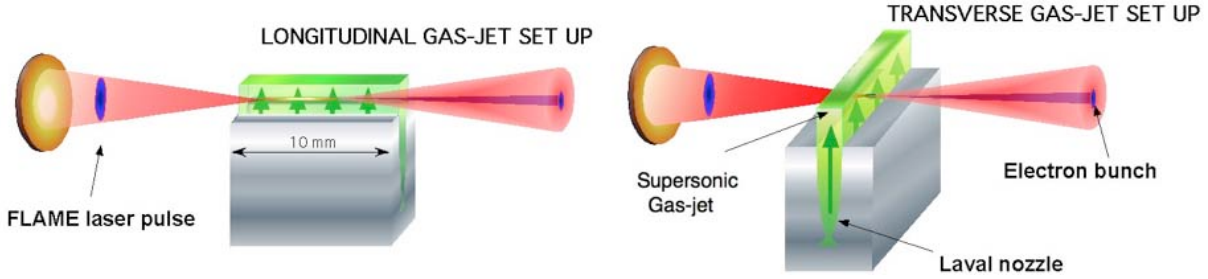

Figure 2.1: Schematic layout of the laser-gas-jet interaction for the production of energetic electron bunches in the self-injection configuration used in the SITE experiment at LNF. We used two different gas-jet length of 10 mm (longitudinal propagation) and 1.2 mm or 4 mm (transverse propagation).

The second SITE run was focused on a more systematic study of the acceleration process for different gas type, gas density using both the transverse and lon- gitudinal gas-jet configurations of Figure 2.1. We used nitrogen or helium with a back pressure ranging from 1 to 17 bar, corresponding to a maximum gas density approximately in the range from 5×10^{18} and 2×10^{19} atoms/cm^3 and a maximum laser-intensity on target of 2×10^{19} W/cm^2 . A total of 3000 shots with e-bunch production was recorded and data were taken with an optical imaging system and Lanex screen placed at 475 mm from the gas-jet to measure both the electron bunch transverse size and, with the insertion of the 50 mm long magnetic dipole at 132.5 mm from the gas-jet, the energy spectrum. In addition, a shadowgraph of the interaction region was taken to measure the longitudinal extent and the transverse

size of the interaction region. The imaging system was set to view the interaction region in the vertical direction, i.e. along the axis perpendicular to the laser polarization plane to image out the Thomson scattered radiation. The plot of Figure 2.2 shows the typical Thomson image obtained from measurements with the longitudinal gas-jet configuration.

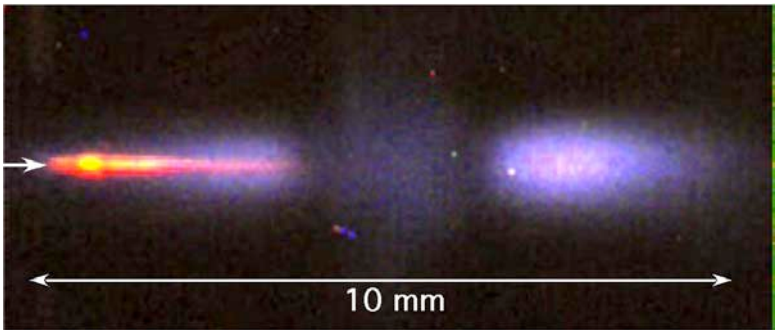

Figure 2.2: Images of the Thomson emission from propagation of the laser pulse in a Nitrogen gas-jet at 10 bar valve pressure. The laser propagates from left to right. Also visible in the image is the plasma self-emission.

As shown by the arrow, the laser propagates from left to right showing a clear Thomson emission (red-yellow in the color figure) in the first 3.2 mm (FWHM) of the propagation. Taking into account the laser beam parameters, we expect a depth of focus of approximately ± 260 μm. Therefore, according to the image of Figure 2.2, laser propagation occurs over a propagation length which is several times the depth of focus. The propagation length was found to be dependent on the gas density and pressure, ranging from approximately 1.3 mm (FWHM) for 70% Nitrogen gas mixture (air) at 1 bar pressure to less than 2 mm (FWHM) for Helium at 15 bar pressure. These results indicate that propagation length increases at higher electron density where stronger refraction effects may occur on the propagation of the laser pulse in the plasma. At this stage we can anticipate possible contribution of self-focusing effects to the observed behavior of the laser pulse. Detailed numerical simulations are in progress [8] for a confirmation of this result.

Information about the accelerated electron bunches was obtained by using the LANEX scintillating screen to measure both the angular divergence and the energy spectrum. The image of Figure 2.3 (left) shows the typical image of a single electron bunch obtained from optimized acceleration in Nitrogen. According to this image, the single bunch exhibits a divergence of approximately 1 mrad FWHM, a value significantly smaller than that measured during the first 2010 SITE run and among the smallest values measured in similar experiments worldwide. The image of Figure 2.3 (right) shows instead the same image integrated over 30 laser shots which gives a overall cone of emission of approximately 10 mrad HWHM. The latter measurement gives an indication of the shot-to-shot pointing stability of the electron bunch. As for the origin of this fluctuation, it is unlikely to be affected by the laser pointing stability which was measured to be within the μrad range. The oscillation of the electron bunch inside the accelerating structure [9] is instead being explored as a possible explanation of the observed limit to the bunch pointing stability.

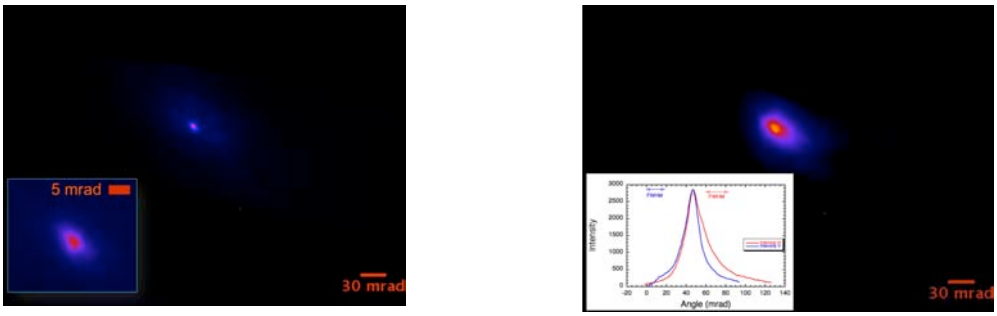

Figure 2.3: Left: Image the scintillating LANEX screen at 47 cm downstream the interaction point showing the bunch transverse size of approximately 0.5 mm and a corresponding bunch divergence of 1 mrad. Right: integrated image of the electron bunch over 30 laser shots showing a total pointing stability of approximately 10 mrad. The bottom-left plot shows the lineout of the image across the vertical and horizontal directions.

Finally, information about the energy of the electron bunch was obtained by inserting the permanent magnet dipole down-stream from the laser focal position. Although analysis of electron spectra is still in progress, at this stage we can anticipate that the measured energy was typically in the range between 50 and 200 MeV, with occasional higher energy events up to the upper limit of the working range of our spectrometer (1GeV). The image of Figure 2.4 shows a typical spectrum of acceleration in Nitrogen in the same conditions of Figure 2.3. The white dot in the centre of the image indicates the average undeflected (no magnet) landing position of electrons.

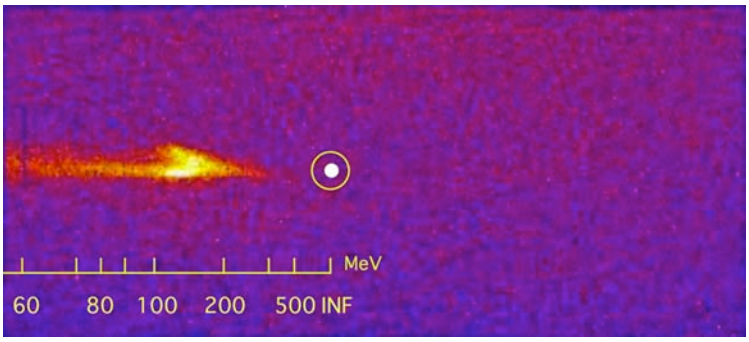

Figure 2.4: Raw spectrum of a typical electron bunch accelerated from a Ni- trogen gas-jet. The spectrum shows a main component above 100 MeV and a low energy tail extending down to 60 MeV. The white dot indicates the landing position of undeflected electron.

In the presence of the magnet, electrons will be deflected on the l.h.s. of the screen according to the dispersion curve of the spectrometer. According to this image, the spectrum shows a main component around 150 MeV and a low energy tail extending down to 60 MeV. This general behavior was quite reproducible from shot to shot and accurate deconvolution of all the spectra is currently in progress to take into account instrumental broadening. These results are being investigated via numerical simulations and the actual acceleration regime operating in our experimental conditions is being identified.

Experimental results obtained during the 2012 self-injection run at FLAME show effective acceleration of highly collimated, high energy electrons up to 1 GeV, with moderate reproducibility and good pointing stability around the 200 MeV energy, a first step for the proposed all-optical radiation source at FLAME.

Acknowledgements

The work was carried out in collaboration with the High Field Photonics Unit (MD.P03.034) and X-ray Photonics (MD.P03.006.006) at INO-CNR partially funded by CNR through the ELI-Italy project and by the MIUR-FIRB SPARX respectively. We acknowledge the CINECA Grant N. HP10CZX6QK2012 for the availability of high performance computing resources and the INFN APE project for the availability of the QUonG cluster.

References

[1] J. Faure et al., Letters to Nature **431**, 541 (2004)
[2] W. P. Leemans *et al.*, Nat. Phys. **2**, 696 (2006).
[3] L.A.Gizzi et al., Nuclear Instr. Methods, B, 2013, in press
[4] L.A.Gizzi *et al.*, Il Nuovo Cimento C **32**, 433 (2009).
[5] L.A.Gizzi, in *Charged and Neutral Particles Channeling Phenomena*, *The Science and Culture Series*, edited by W. S. Publishing (2010).
[6] T. Levato *et al.*, in *Laser-Plasma Acceleration*, International School of Physics "Enrico Fermi", edited by F.Ferroni and L.A.Gizzi (IOS Press, 2011), Vol. CLXXIX.
[7] L.A.Gizzi, Technical report, INFN and CNR-INO (unpublished).
[8] F. Rossi *et al.*, AIP Conference Proceedings **1507**, 184 (2012).
[9] K. T. Phuoc *et al.*, Phys. Rev. Lett. **97**, 225002 (2006). [44]

3 LILIA experiment

M.P. Anania (Ass. Ric.), L. Cacciotti (Tecn.), D. Di Giovenale (Art. 23) G. Di Pirro, A. Drago, G. Gatti, R. Sorchetti (Tecn.), F. Villa (Ass. Ric.).

Participant institutions: other INFN sections (Mi (C. De Martinis (Resp. Naz) , RM1, RM2, Bo, Pi, LNS), CNR-INO-Pisa

NTA-LILIA is an experiment of light ions acceleration trough laser interaction with thin metal targets to be done at the FLAME facility, which is now running in Frascati. LILIA, in particular, is finalized to study, design and verify a scheme which foreseen the production, the characterization and the transport of a proton beam toward a stage of post acceleration (high frequency compact linacs). Now the maximum operating laser intensity is limited to 10^{19} W/cm^2 due to the lack of a parabola with a focal length shorter that the current used. In this configuration, according to the interaction theory by short pulse laser and to performed numerical simulations, we expect a proton beam with maximum energy of a few MeV and a number of proton/shot up to 10^{10}-10^{12}.

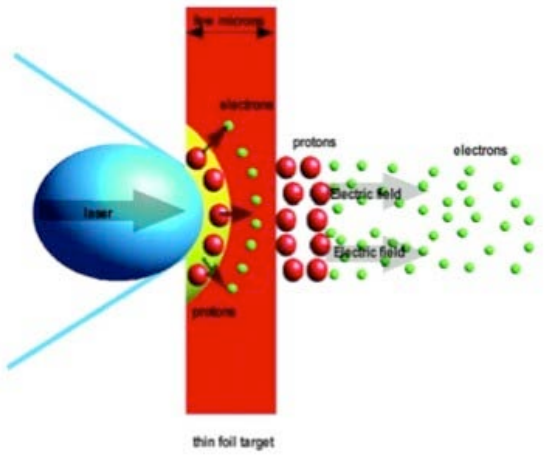

Figure 3.1 Schematic representation of the proton acceleartion experiment

In the majority of experiments for proton accelerations, the regime occurring is the so called TNSA (Target Normal Sheath Acceleration). The laser pulse heats the electrons and ionizes the medium. Next the electrons diffuse around the target building an intense electric field. This field accelerates the free protons present on the target surfaces, both in the forward direction (from the rear side) and in the backward direction (from the front surface).

The FLAME facility has been fully operational in the middle of 2012 for the first test experiments of electron Laser Wakefield Acceleration (LWFA). At the end of October 2012 it was possible to install the components for the proton acceleration experiment (LILIA).

As of now the maximum laser intensity is limited to 10^{19} W/cm^2 due to the lack of a parabola with focal length shorter than the present one. In this configuration, according to performed numerical simulations, we expect a proton beam with maximum energy of few MeV (10 MeV is as of now the maximum energy allowed by the local authorities for the place where the experiment will be located) and total intensities up to 10^{10}-10^{12} protons/shot. Although these values are modest compared to the present state of art, nevertheless their scientific relevance is very important due to the fact that we will have, with a reasonable effort, a real laser driven source that will play the role of a test facility as far as emission process control and repeatability and post acceleration studies will be involved. In LILIA phase I we plan to perform a parametric study of the correlation of the maximum TNSA accelerated proton energy, with respect to the following parameters:

- Laser pulse intensity (in the range $10^{18} – 5\ 10^{19}$ W/cm^2)
- Laser pulse energy (in the range 0.1-5 J)
- Laser pulse length (in the range 25 fs- 1ps)
- Metallic target thickness (in the range 1-100 μ).

In such a frame we would like to deeply investigate the experimental scale rules within the possibilities offered by the FLAME facility. Moreover, this will provide the opportunity to get experience in the development of diagnostic techniques and in target optimization. The possibility to produce a real proton beam able to be driven for significant distances (50-75 cm) away from the interaction point and which will act as a source for further accelerating structures will be also investigated.

When FLAME phase II performances will be available (Short focal length OA Parabola: waist≈2.5μ, $I \approx 10^{21} W/cm^2$, we might select a bunch at E = 30 MeV with a narrow spread ΔE and still have a reasonable number of protons (10^7 ~ 10^8). This opens a very interesting perspective for applications such as hadrontherapy in connection with a post-acceleration stage in order to reach energies up and beyond 100 MeV. Indeed if a sufficient current intensity can be reached at 30 MeV with a narrow spread ΔE/E ~ 1% and a good beam quality after transport, energy selection and collimation, the protons bunch might be post-accelerated after injection in a high field linac (Figure 3.2), as the one developed for the INFN ACLIP project (suitable for medical applications)

The LILIA experiment has been designed to be housed in the interaction chamber available at the exit of the laser compressor in the FLAME bunker. The layout of the first phase of the experiment is shown in Figure 3.2 and 3.3 and it foresees:

- a special designed optical breadboard, with standard metric holes format, to allow the definition of a common reference plane level and the assembly of components within the chamber;
- a multi shot target holder able to be remotely moved in x-y-z directions and rotated along the z-axis with respect to the laser beam. This will allow a very accurate positioning of the targets with respect to the laser beam and the possibility to perform multi shot experiments without having to open the vent of the chamber to replace the already used targets. The target holder has been designed for the use of aluminium foils (pure up to 99.0%) with thickness as low as *1 μm*and the possibility to provide up to 30 usable shots. The position accuracy of the targets with respect to the laser beam is of the order of *20 μm* for the translation stages and of 0.1 degrees for the rotation stage. The alignment of the targets with respect to the power laser beam will be accomplished using alignment lasers and devoted optical windows in the chamber;
- a remotely movable multi-detector holder able to house 8 stacks of radio-chromic detectors to be used close (*50 mm*) to the interaction point. A fixed lead foil (*3 mm* thick) is used to avoid the damage of stacks adjacent to the one of interest for a specific laser shot;
- the availability of multiple detectors copes with the possibility to perform multiple experiments on different targets in a very short time, minimizing the fluctuations in the laser beam characteristics;
- a more accurate analysis of the energy distribution of the produced ions will be carried out at a fixed emission angle with a Thomson parabola (TP) spectrometer with its related detectors. A *150 mm* diameter vacuum movable window in the interaction chamber at an angle of 120 degree with respect to the laser beam will allow the positioning of the TP.

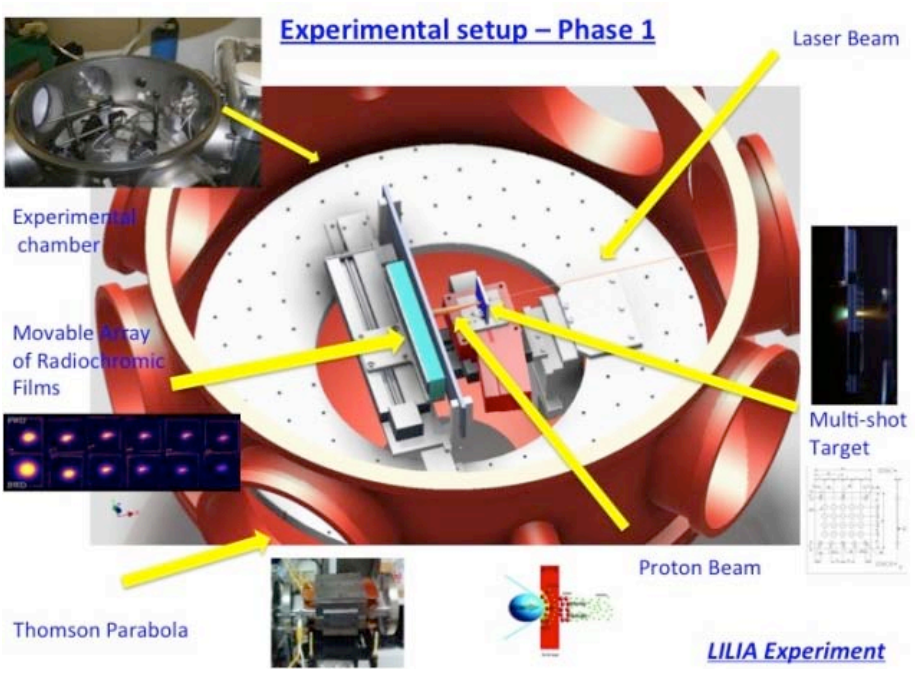

Figure 3.2 Sketch of the LILIA mechanical setup

During autumn 2012 the mechanical set up has been installed and aligned in the interaction chamber. The FLAME beam has been focused on the target and preliminary test have been carried out during two shifts in October and December 2012. During these tests we were limited for technical problems in the laser power that was of the order of 2 joules. Nevertheless we have obtained the first experimental evidence of proton acceleration.

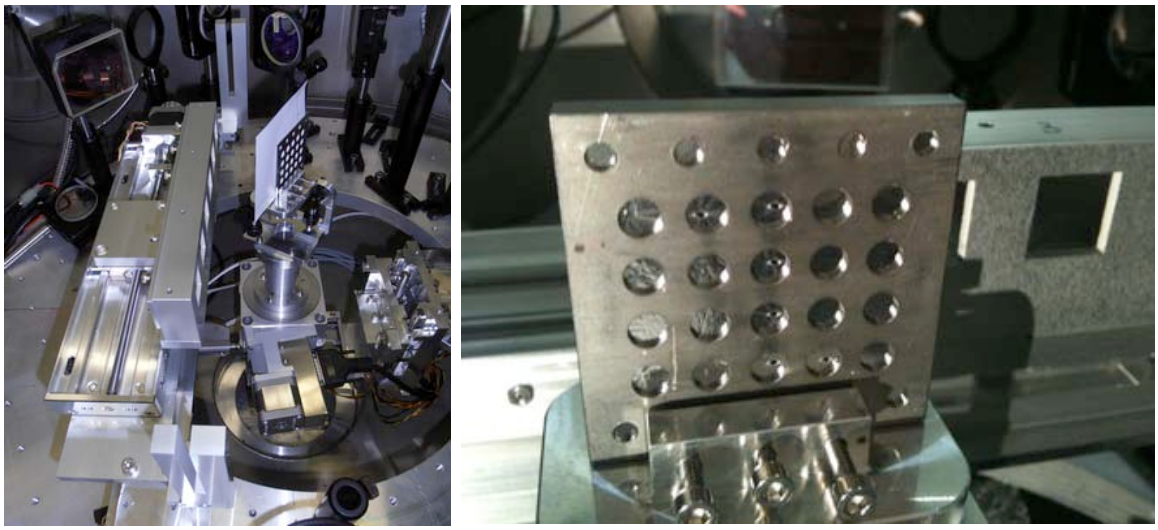

Figure 3.3 The remotely movable radio-chromic detectors and the multi-shot target holder

Behind the multi-shot target two different detectors are placed: an a EBT3 radio-chromic film by Gafchromic films or a CR-39 plastic polymer. The Figures 3.4 and 3.5 show the first pictures of the EBT3 and CR-39 impressed by protons emitted from a 3 μm Al target with a 1.5 Joule laser shot.

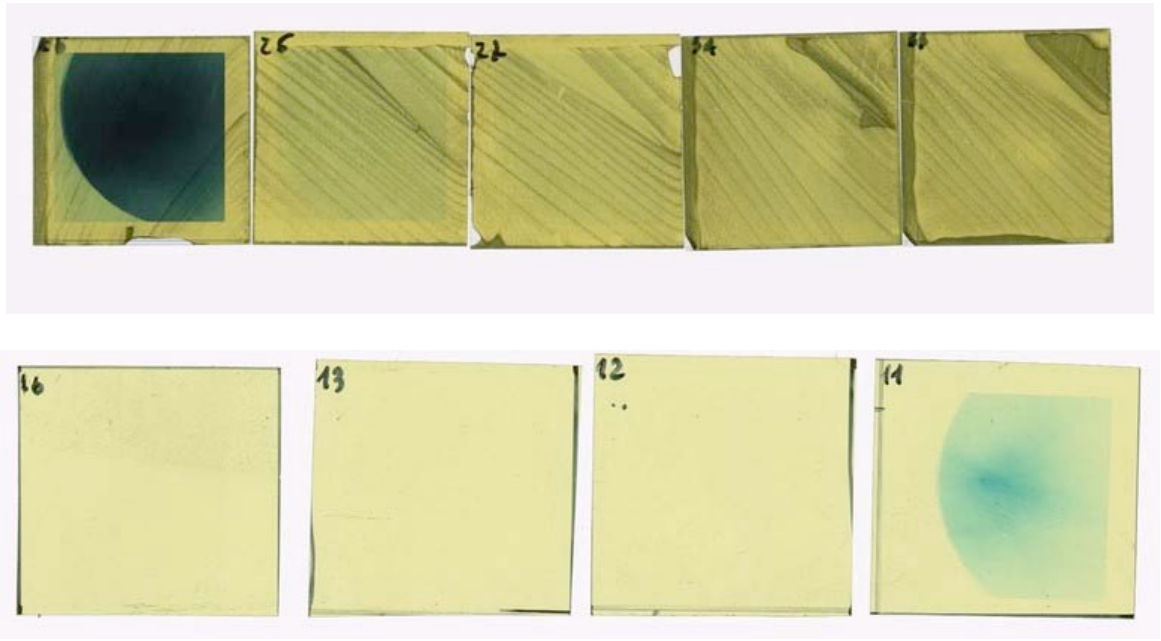

Figure 3.4 Impressed EBT3 radio-chromic films

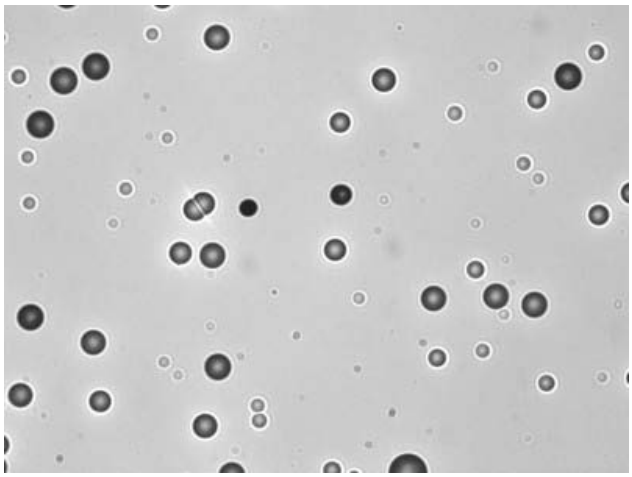

Figure 3.5 Impressed CR39 film

The radio-chromic detector was shielded by a 6 μm thick aluminium foil in order to protect it by the light emission during the laser interaction.

By the obtained results we can derive a lower limit for the maximum energy of the emitted protons of at least 1.6 *MeV*. A detailed analysis of the acquired data is now underway.

References

[1] A. Bacci, D. Batani, G.P. Cirrone, C. De Martinis, D. Delle Side, A. Fazzi, D. Giove, D. Giulietti, L. Gizzi, L. Labate, T. Levato, P. Londrillo, M. Maggiore, L. Martina, V. Nassisi, M. Passoni, A. Sgattoni, L. Serafini, S. Sinigardi, G. Turchetti, L. Velardi, "Laser induced proton acceleration at the FLAME facility in Frascati: LILIA experiment", Atti del II Workshop Plasmi, Sorgenti Biofisica ed Applicazioni, Lecce, 26 Ottobre 2010, Edizione Coordinamento SIBA, ISBN 978-88-8305-087-9 (print version), (2011)

[2] M. Ferrario et al. "Recent Results at the SPARC_LAB Facility" Proceedings of IPAC2012, New Orleans, Louisiana, USA

[3] L.Serafini, A.Rossi, A.Bacci, M.Ferrario, P.Tommasini, C.De Martinis, "Status of the Project PLASMONX and the experiment LILIA" Proceedings COULOMB'11:Optical Acceleration of Ions and Perspectives for Biomedicine. November 4-5 2011 –Bologna – in press

[4] V. Nassisi, D. Delle Side, L. Velardi, G. Buccolieri, F. Paladini, D. Giove, C. DeMartinis, A.Fazzi. High voltage pulse of short duration to feed solenoids for intense ion beam transport. IIIWorkshop Plasmi, Sorgenti, Biofisica ed Applicazioni, Lecce 19 Ottobre 2012

[5] G.Turchetti, S.Sinigardi, P.Londrillo, F.Rossi, D.Giove, C.De Martinis, "Transport and energy selection of laser generated protons for postacceleration with a compact linac " accepted for publication as a Regular Article in Physical Review Special Topics- Accelerators and Beams.

4 THOMSON experiment

C. Vaccarezza (Resp. Naz.), M.P. Anania (Ass. Ric.), M. Bellaveglia (Art. 23), M. Cestelli Guidi (Art. 23) , D. Di Giovenale (Art. 23) G. Di Pirro, A. Drago, M. Ferrario, A. Gallo, G. Gatti, A. Ghigo, A. Marcelli, E. Pace, L. Palumbo (Ass.), F. Villa (Ass. Ric.).

Participant institutions: other INFN sections (Mi, RM1, RM2, Ba, Ca, Pi, Ts, Fe, Le, Fi, Na, LNS), ENEA-Frascati

In the 2012 the SL-Thomson project has seen the completion of the procurement of the hardware foreseen for the interaction region. The Thomson source installation will be completed by February 2013 and the electron beam line commissioning will take place in March, while the photon beam transport optimization will be addressed in April 2013 and the collisions are expected soon after.
The SL-Thomson project foresees the realization of a monochromatic source of ultra-fast X-ray pulses by Thomson back-scattering (TS): the key points of this configuration are the flexibility and the potential compactness with respect to conventional synchrotron sources.
The TS source driven by the SPARC photoinjector high-quality electron beam will be able to work in the high-flux- moderate-monochromaticity-mode(HFM2), in the moderate-flux- monochromatic-mode (MFM) and in the short-and-monochromatic-mode (SM).

The first experiment to take place will be BEATS2 [1] with the source operating at high flux.

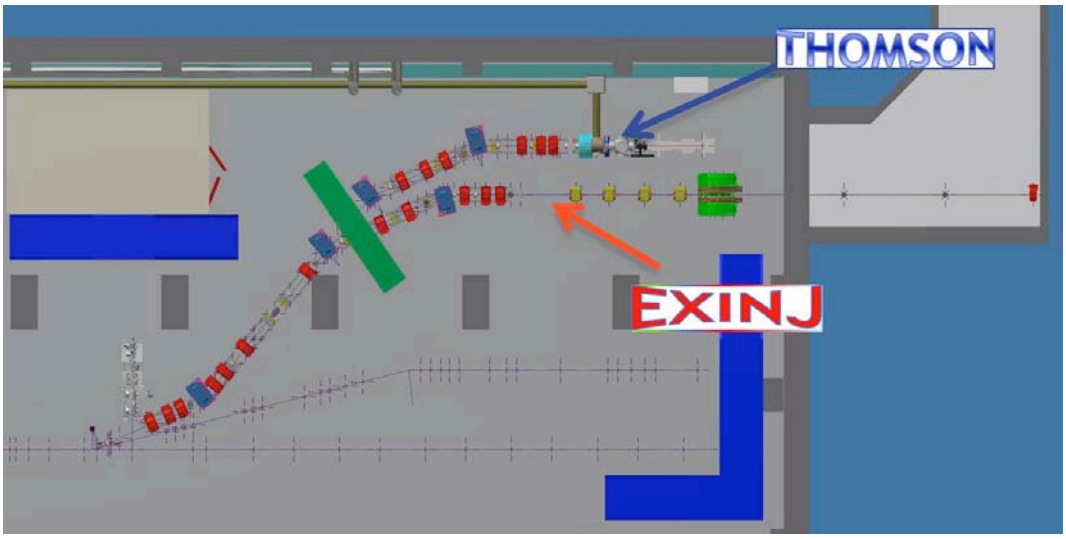

Figure 4.1 CAD drawing of the Thomson and Exinj electron beam transfer lines layout.

The installation of the electron and photon beam lines up to the Thomson Interaction Point has been almost completed in 2011, while in 2012 the interaction chamber setup has been finalized and procured together with the 1.2 T solenoid magnet for the final focusing at low energy.
The electron beamline brings the electron beam from the photoinjector to the interaction point where the laser pulse coming from the FLAME laser system arrives through a dedicated photon beamline. In this configuration the electron beam energy can range from 28 MeV up to 150 MeV, and the electron beam transport is meant to preserve the high brightness at the linac exit and to ensure a very tight focusing and a longitudinal phase space optimization for the whole energy span.
The electron beam parameter list for the two interaction points are reported in Table 1. In Figure 4.1 the machine layout is shown, where the electron transfer line departs from a three way vacuum chamber inside the first dipole downstream the RF deflector that is used for the six-dimensional phase space analysis of the SPARC beam.

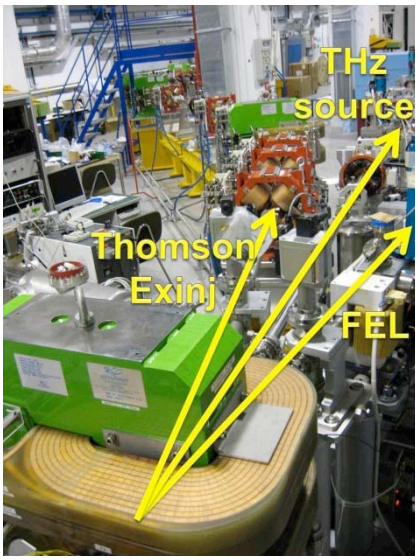

Figure 4.2 Three-way branch for the FEL, THZ and Thomson-Exinj beamlines.

This dipole is also part of the chicane foreseen for the seeding configuration of the SPARC FEL undulator (straight direction downstream the photoinjector) and of the 14° degrees dogleg that brings the electron beam up to the SPARC Therahertz source, see Figure 4.2

Table 1 Electron beam parameters at the Thomson source interaction point

Parameter	Value
Bunch charge (nC)	**0.2 ÷ 1.0**
Energy (MeV)	28 ÷150
Length (ps)	15 ÷ 20
$\varepsilon_{n\ xy}$ (mm mrad)	1 ÷ 5
Energy spread (%)	0.1 ÷ 0.2
Spot size at interaction point rms (mm)	05 ÷ 20

The electron beamline consists in a 30 m double dogleg ending in a two branch beam delivery line that provides two separate interaction regions: the outer one from the photoinjector is dedicated to the Thomson Source. The total beam deflection is about six meters from the photoinjector and undulator axes. A total of six rectangular dipoles and 19 quadrupoles have been installed in 2011 to drive the electron beam up to the two IPs.
From the magnetic measurements results all the dipoles show a relative magnetic length deviation of about 0.1 %, while at the nominal current the deviation from the Tosca 3D code evaluation is around 1% within a good field region of ±10 mm in both x and y directions.
In place of the foreseen dumping dipole, not yet delivered, an existing dipole will be used to dump the electron beam inside the well off in the floor of the hall; this will limit at the beginning the beam energy up to 90 MeV for the Thomson experiment. The well off aperture is able to host the two electron trajectories: the 14° nominal one from the designed dipole and the 25° trajectory from the temporary solution see Figure 4.3.

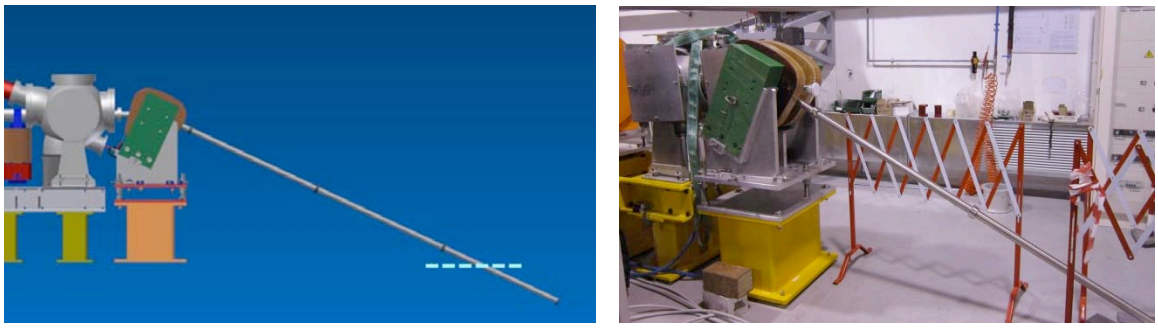

Figure 4.3: Temporary dumper solution realized with an existing dipole mounted downstream the parabolic mirror location, while the nominal position of the ad hoc designed dipole is downstream the short interaction tee vacumm chamber.

Nine over a total of thirteen Beam Position Monitors (BPM) have been installed for the first phase of the Thomson beamline commissioning; together with three high resolution beam imaging setup they will provide the necessary beam diagnostic for the orbit correction and beam phase space measurements. Each BPM device is equipped with a readout electronics based on the Libera four single pass processors from Instrumentation Technology .

The Thomson Interaction vacuum chamber has been delivered at the end of 2012, see Figure 4.4, the setup consists in two mirror stations that will determine the in & out trajectory of the photon beam (red path in the figure), plus an interaction chamber in the middle that also hosts the diagnostic for both the electron and photon beams. After the first phase of the commissioning devoted to the tuning of the electron beam, the foreseen parabolic mirror will be installed downstream the interaction point on a movable support table remotely controlled. The mirror will be able to focus the photon beam at the IP down to a 10 μm spot size.

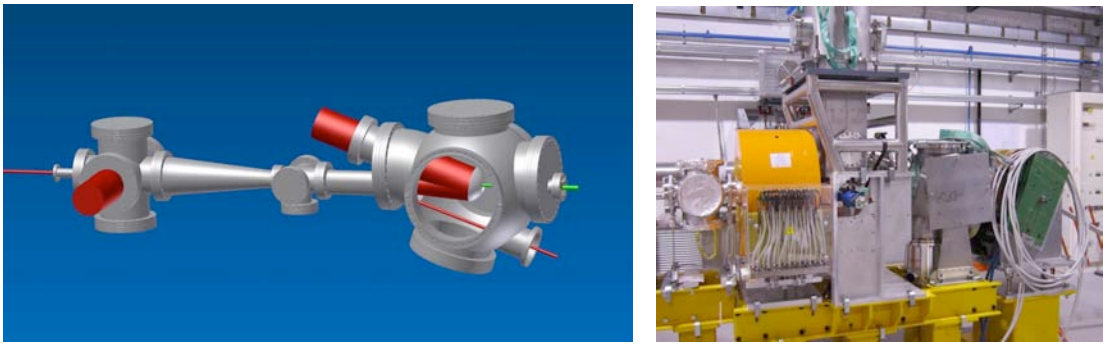

Figure 4.4: The Thomson IP vacuum chamber setup: lefte the CAD drawing of the system with the path of the laserright the interaction chamber as mounted in the beamline.

The actual Thomson interaction chamber is the central tee-vacuum chamber where a double screen movement is mounted to get the imaging of the electron and photon beam at the IP, Figure 4.5. The double screen setup consists in an OTR plus a YAG screen with two mirrors oriented in such a way to recoil the image of the two beams coming from the opposite directions.

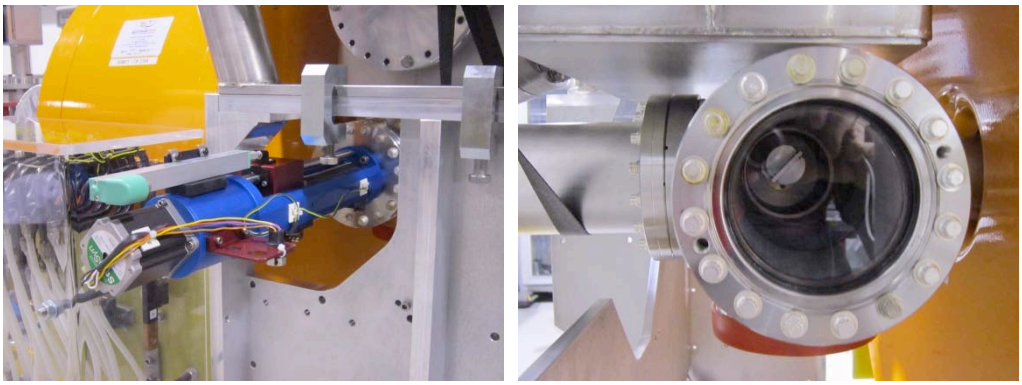

Figure 4.5: The Thomson IP electron-photon diagnostic system

The laser beam transfer line from FLAME to the Thomson interaction region is composed by a series of high reflectivity mirrors inserted in a vacuum pipe 50 m long. The mirrors, 8 inches diameter, are supported by motorized gimbal mounts in order to assure the alignment up to to the off-axis parabola that focuses the laser pulse on the electron beam, see Figure 4.6.
At the entrance of the photon beam line in the SPARC bunker a concrete wall has been realized in order to stop any radiation draft from the FLAME area towards the SPARC bunker, and to allow people entering in the SPARC hall during the FLAME laser operation and viceversa. The vacuum of the photon beam line is a the level of 10^{-6} *Torr* and suitable for the transport of the compressed laser

pulse ~10 *fs* length as needed for the plasma acceleration experiment. In Table 2 the laser pulse parameters are reported as foreseen for the Thomson Source application.

Table 2 Laser beam parameter list

Parameter	Value
Wavelength (nm)	800
Compressed pulse energy(J)	5
Pulse duration/bandwidth (ps/nm)	3÷12(80)
Rep.Rate (Hz)	10
Prepulses contrast	$>10^6$
Contrast ratio at 1 ns before (ASE)	$>10^8$
Contrast ratioat 1–100 ps before	$>10^6$
Contrast ratio of replica	$>10^5$
Beam quality M^2	↕1.5
Energy stability (%)	10
Pointing stability (μm)	< 2
Synchronization with SPARC clock (ps)	<1

The Thomson scattering experiment needs an extremely precise synchronization between electron bunch and laser pulse. The relative time of arrival jitter of the two beams is fundamental to obtain a repeatable and efficient interaction. The electrons and photons have to be synchronized with a relative jitter < 500 *fs*. This can be obtained with a standard electrical distribution of the reference signal, already present at SPARC. Anyway an optical distribution is preferable to obtain precise time of arrival measurement resolution (equal or less than 5 *fs*) and to obtain better synchronization between the two beams. This can be achieved by means of an optical cross-correlation between short laser pulses (100÷200 *fs*). In particular the electrical (or optical) master oscillator in our project will serve two laser oscillator clients: SPARC photo injector for the production of electrons and FLAME laser for the production of the high intensity pulse for the Thomson interaction.

The RF system phase will be also locked to the master oscillator using low noise phase detection; and the phase feedback loops will be implemented too. They can be divided in two general types: slow (bandwidth <10 Hz) and fast (10 Hz to some MHz bandwidth). The formers are used typically to compensate slow drifts caused by thermal elongation of cables and are implemented by means of high resolution stepper motors. The others are designed to compensate the high frequency noise suffered by the systems that is normally due to mechanical vibrations or electrical noise in the RF circuits or power amplifiers (klystron tubes and driver amplifiers).

In 2012 the activity of the BEATS2 [2] group has been joined to the SL-Thomson Source due to the synergy between the first phase of the experiment devoted to the calibration of the detector systems and the collision phase of the source commissioning devoted to the characterization of the X-ray radiation.

In the first months of the 2012 the calibration of the diode-scintillator systems has been performed with quasi-monochromatic x-ray beam in the range 16-24 keV at the Larix laboratories, Ferrara University; at the same time the response of such a system has been studied for x-ray energies >500keV, together with an imaging system for the same energy range. From summer to the end of 2012 the procurement of this high energy radiation diagnostic system has been carried on together with the first measurements of background activity in the SPARC LAB bunker during the machine runs.

According to the SPARC-LAB approved schedule for 2013 the commissioning of the Thomson source is foreseen to start in March 2013 with the following steps:

Figure 4.6: SL-Thomson laser transfer lines inside the SPARC bunker (left). Motorized mirror vacuum chamber (right).

a) Phase 1: electron beam line commissioning that foresees a 200 pC beam at the energy of 80 MeV and 30 MeV that will be focused at the IP by means of the final quadrupole triplet only.
b) Phase 2: Photon beam line commissioning at high power with synchronization system tuning for first collisions and characterization of the first obtained radiation.
c) Phase 3: electron beam focusing at 30 MeV by means of the 1.2 Tesla solenoid to get the tight focusing of the beam with charge Q=0.3 ÷ 1 nC .
d) Beats2 experiment tuning and data taking.

Publications in 2012

- C. Vaccarezza, "Thomson_radiation_source\& applications", Joined IZEST - Helmholtz Beamlines Workshop, GSI - Darmstadt - Germany, April 23-25, 2012
- Paolo Cardarelli *et al*, "Energy distribution measurement of narrow-band ultrashort x-ray beams via K-edge filters subtraction", Appl. Phys. 112, 074908 (2012), DOI:10.1063/1.47
- "Characterization of a "PIN diode-scintillator" detector for the measurement of pulsed x-ray beam flux in the range 16-24 keV", Bachelor Thesis: F. Forlani. Supervisors: Prof. M. Gambaccini, P Cardarelli. Università diFerrara, March 2012

References

[1] P. Oliva et al., Nucl. Instr. Meth. A 615 93-99, (2010)
[2] http://www.ba.infn.it/beats/

5 EXIN experiment

M.P. Anania (Ass. Ric.), E. Chiadroni (Ric.), D. Di Giovenale (Art. 23), G. Di Pirro (Resp.), M. Ferrario, A. Gallo, G. Gatti, A. Ghigo, E. Pace, C. Ronsivalle (Ass.), S. Tomassini,C. Vaccarezza, F. Villa (Ass. Ric.)

Participant institutions: other INFN sections (Mi (L. Serafini -Resp. Naz.), RM1, RM2, Pi, Na,), CNR-INO-Pisa

The external injection experiment at SPARC LAB aims at combining the high accelerating gradient characteristic of plasma-based accelerators with the production of high quality, stable and reproducible beams, typical of conventional RF linear accelerators. In terms of electron beam parameters, the target beam, after acceleration, possesses a low normalized emittance (a few mm mrad), short time duration (a few tens of fs) and an energy spread of less than 1%. Such high quality electron bunches can actually enable a variety of applications of plasma accelerators, such as front-end injectors for conventional accelerators and drivers for compact, short-pulse radiation sources.

Plasma accelerators are based on the excitation of large amplitude waves (or wakes) in a plasma; they can be driven by laser pulses [1] (LaserWakeField Acceleration , LWFA) or by particle bunches [2] (PlasmaWakeField Acceleration, PWFA). The driver first displaces plasma electrons while propagating in the plasma; the subsequent oscillation of the plasma creates a plasma wave (a wake) following the driver. The accelerating field of the wake depends on the unperturbed plasma density and can reach a value of several GV/m, up to 1 TV/m in some regimes.

The route to external injection experiment can be logically divided into two parts. The first one concerns the generation and acceleration of proper high brightness electron beam up to the injector end. The second part consists in the design, realization and commissioning of the transport lines down to the interaction chamber with the plasma wave and the subsequent diagnostic stations. The electrons and high power laser pulse transport lines installations are underway, while the engeneering of the interaction chamber is ongoing.

The main goal of the experiment is to produce in a stable and reproducible way a beam with a charge of few tens of pC, an energy up to 1 GeV with a spread less than 1% and a normalized emittance of few mm-mrad. High accuracy and precision diagnostic tools are compulsory for both transverse and longitudinal characterization of the electron beam; preferably non intercepting and single shot diagnostics, whenever available, should provide the required resolution of few tens of fs bunch length and few microns transverse beam size.

At SPARC LAB a wide energy range spectrometer will provide means of measuring the beam energy and its spread. The emittance constitutes a much harder parameter to measure: a possible candidate is the quadrupole scan technique, tough, if the beam energy spread is relatively large, the results could be unreliable due to chromatic effects [3]. As for the longitudinal diagnostics, we will insert an RF deflector downstream the plasma interaction chamber. Finally, a device to measure the betatron radiation and the coherent transition radiation is foreseen, to gain knowledge on many parameters of the accelerating process [4].

The high brightness beam needed to feed the plasma wave must be short compared to the plasma wavelength λp ($\lambda p > (30 - 40)\sigma z$), in order to prevent an excessive correlated energy spread after plasma interaction, since we plan to operate the plasma accelerator in a linear to mildly non-linear regime. This choice comes from the need to prevent the possibility of self-injecting spurious charge, which can happen in the bubble regime. To ease the task, the plasma wavelengths should be in excess of 100 μm, meaning plasma densities up to 10^{17} cm^{-3}. The expected accelerating fields can then be estimated to be of the order of few tens of GV/m. To meet the desired energy it is then necessary to guide the driving laser pulse over a length which is much greater then its natural one. There are two main strategies for achieving guiding: either by transverse tapering of the plasma density (n_0 / r^2) or by using a capillary as an optical waveguide [5]. Transverse tapering, though harder to properly manage, has the advantage of preventing any laser energy leakage from the plasma channel, allowing a longer acceleration; on the contrary, the capillary waveguide is easier to operate but, due to losses at the dielectric boundaries, allows acceleration lengths up to 6 - 8 cm (assuming a glass capillary) and severely constrains the laser spot-size w_0 and focus position [6]. We will employ both techniques, at least for the first part of the external injection experiment.

Preliminary simulations, have benn berformed using the code QFLUID2, a cylindrical code that uses fluid approximation and QSA for plasma currents [7]. Since the needed input bunch length is very demanding, a first set of simulation using ELEGANT [8] has been run in order to asses its feasibility. A 0.5-1 nC, 5 ps long bunch has been simulated from SPARC photo-cathode to interaction chamber. During the transport it has been compressed by velocity bunching and/or magnetic compression and longitudinally tailored by a slit collimator, after dispersion by means of the SPARC RF deflector. The produced beams had a length down to 7 μm, a charge in the range of 5-20 pC and emittance under 1 mm − mrad. Even if the length requirements were not met yet, such beams have been injected and accelerated in the capillary using QFLUID2. The transverse and longitudinal phase spaces of the accelerated beam are shown in figure 5.1 while figure 5.2 reports a slice analysis. The beam parameters are summarized in Table 1.

Charge	5 pC
Energy	570 MeV
$\Delta\gamma/\gamma$	2.70%
ε_n	1.4 mm-mrad

Table 1: Beam parameters for capillary laser guiding

The plasma density is 10^{17} cm^{-3}, the acceleration length is 8 cm and the capillary inner diameter is 100 μm. It is clear how the input bunch excessive length prevented to reach the desired performance in energy spread and final energy. These working conditions should be considered intermediate, easier steps toward the target parameters reported before that will be met when shorter bunches will be available.

In order to reach the required bunch length, numerical studies are underway foreseeing to directly produce a short, low charge bunch from the photo-cathode, which will be then compressed by velocity

bunching and, if needed, magnetic compression and a collimator. With such beams it seems to be possible achieving the desired beam energy and quality.

For preventing a huge normalized emittance dilution after the bunch leaves the plasma [9], a proper matching at plasma entrance end exit must be enforced [10]. This can be done by focussing the laser inside the plasma and by guiding its defocusing after acceleration.

Another problem arises when trying to increase the bunch charge: since the focusing forces inside the plasma waves are very intense, the beam transverse equilibrium size is small and the bunch density can become comparable to the plasma's. When this happens the electron beam becomes the driver of another plasma wave, loosing energy to the plasma instead of gaining it.

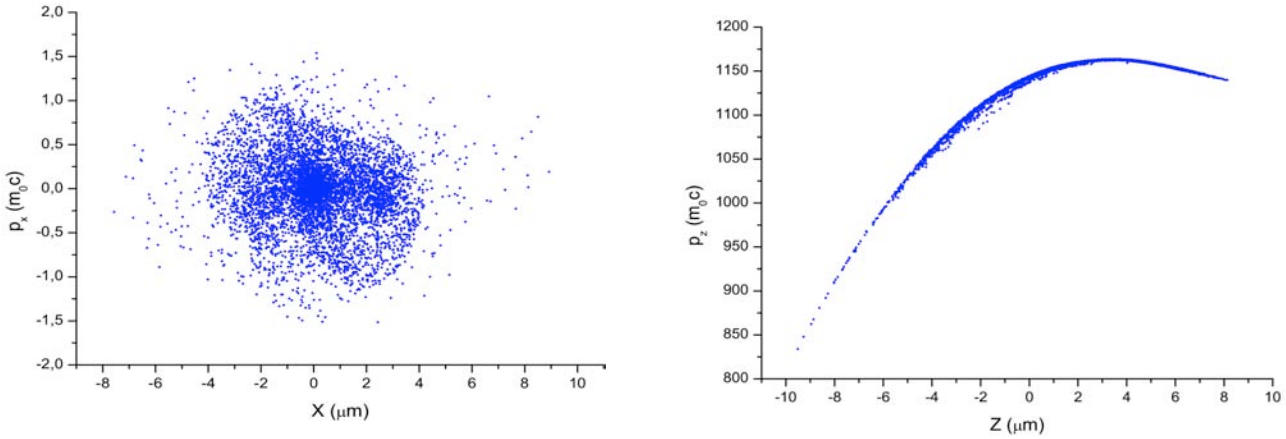

Figure 5.1: Phase spaces of the accelerated beam.

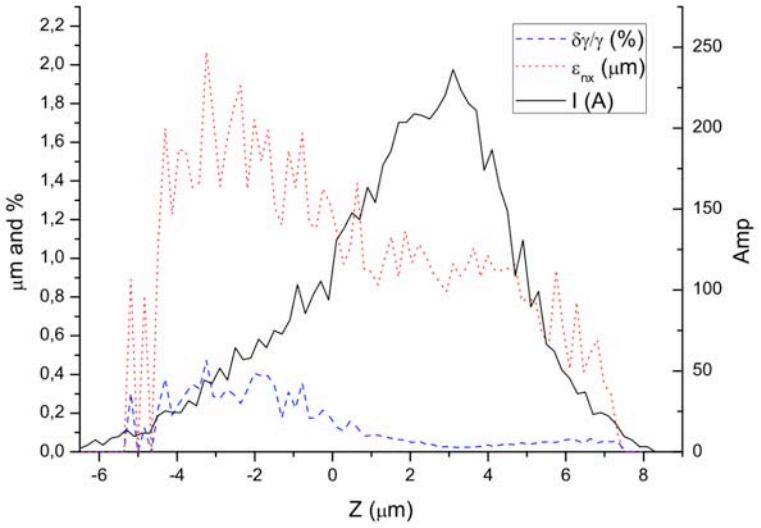

Figure 5.2: Slice analysis of the accelerated beam.

Publications in 2012

- A.R. Rossi, Plasma Acceleration Experiment at SPARC_LAB with External Injection, International Particle Accelerator Conference, poster session, New Orleans, USA.
- Mostacci et al., Phys. Rev. Spec. Top. Acc. & Beams **15**, 082802 (2012).
- M. Migliorati et al., Phys. Rev. Spec. Top. Acc. & Beams **16**, 011302 (2013).
- P. Antici et al., J. App. Phys. **112**, 044902 (2012).
- Cianchi et al., NIM A, in press.

References

[1] E. Esarey, C.B. Schroeder and W.P. Leemans, Rev. Mod. Phys. **81**, 1229 (2009).
[2] P. Muggli et al, in Proc. of 2011 Particle Acc. Conf., New York, NY, USA, TUOBN3.
[3] A. Mostacci et al., Phys. Rev. Spec. Top. Acc. & Beams **15**, 082802 (2012).
[4] S. Corde et al., Plasma Phys. Control. Fusion **54**, 124023 (2012).
[5] F. Wojda et al., Phys. Rev. E **80**, 066403 (2009).
[6] N. Cross et al., Phys. Rev. E **65**, 026405 (2002).
[7] See the presentation by P. Tomassini available at http://agenda.infn.it/getFile.py/access?resId=0&materialId=slides&confId=3444.
[8] M. Borland, in *Proceedings of the* 6th *International Computational Accelerator Physics Conference*, Phys. Rev. Spec. Top. Acc. Beams **4**, 070701 (2001).
[9] M. Migliorati et al., Phys. Rev. Spec. Top. Acc. & Beams **16**, 011302 (2013).
[10] M. Ferrario in *Proceedings Of The International School Of Physics, Enrico Fermi, Course CLXXIX - "Laser-Plasma Acceleration"*, (2011).
[11] P. Antici et al., J. App. Phys. **112**, 044902 (2012).
[12] A. Cianchi et al., NIM A, in press.

6 COMB experiment

M. Ferrario (Resp. Naz.), D. Alesini, M.P. Anania (Ass. Ric.), F. Anelli (Art. 15), M. Bellaveglia (Art. 23), L. Cacciotti (Tecn.), M. Castellano (Ass.), E. Chiadroni, D. Di Giovenale (Art. 23) G. Di Pirro, G. Gatti, A. Ghigo, M. Migliorati (Ass.), A. Mostacci (Ass.), E. Pace, R. Sorchetti, F. Villa (Ass. Ric.).

Participant institutions: other INFN sections (Mi, RM1, RM2, Bo, Pi, Na), CNR-INO-Pisa

In laser COMB operating mode the SPARC photocathode is illuminated by a comb-like laser pulse to extract a train of electron bunches which are injected into the same RF bucket of the gun. The SPARC laser system, based on a Ti:Sa oscillator has been upgraded for this specific application. The technique used relies on a α-cut beta barium borate (α-BBO) birefringent crystal, where the input pulse is decomposed in two orthogonally polarized pulses with a time separation proportional to the crystal length. In the first accelerating structure operating in the VB mode, i.e. injecting the bunch train near the zero crossing of the RF wave, the bunch train is compressed by the longitudinal focusing effect of the RF wave and with a proper choice of injection phase is possible to keep under control both the intra-bunch distance as well as the single bunch length. This method preserves all the extracted charge and it is different from other passive tecniques [1], where the train is produced by using a mask that

stops a significant fraction of the charge. Up to four electron beam pulses shorter than 300 fs and separated by less than 1 ps have been characterized and a narrowing THz spectrum produced by the bunch train has been measured [2]. In addition two electron beam pulses have been injected in the undulator and a characteristic interference spectrum produced by the FEL interaction in this new configuration has been observed, confirming that both pulses have been correctly matched to the undulator and were both lasing [3]. Coherent excitation of plasma waves in plasma accelerators [1] can be also performed with this technique. Preliminary simulations [4] shown that a train of 3 electron drive bunches, each of them 25 mm long, with 200 pC at 150 MeV and 1 mm rms normalized emittance, could accelerate up to 250 MeV a 20 pC, 10 mm long witness bunch, injected at the same initial energy in a 10 cm long plasma of wavelength 383 mm. As shown in figure 6.1 the drive bunches will loose energy to excite the plasma accelerating field up to 1 GV/m in favour of the witness bunch. Simulations show also that the witness bunch can preserve a high quality with a final energy spread less than 1 % and 1.6 mm rms normalized emittance. A test experiment is foreseen at SPARC_LAB, aiming to produce a high quality plasma accelerated beam able to drive a FEL in the SASE mode.

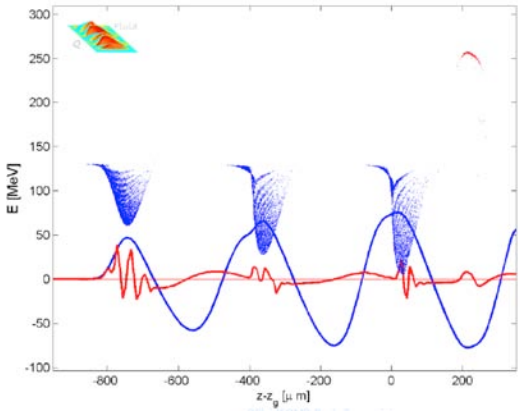

Figure 6.1: Longitudinal phase space of the COMB beam at the end of the acceleration process. The accelerating field is also plotted in arbitrary units.

A specific tool able to make precise measurements of the temporal profile of extremely short electron bunches is needed for a detailed understanding of the bunch length and, in the framework of SPARC_LAB, it has been identified in the Electro-Optical Sampling (EOS). Single-shot electro-optic (EO) detection techniques are ideally suited for this purpose since they are nondestructive and can be carried out concurrently during regular operation of the PWFA experiments. An important aspect is that they permit correlation studies between the measured time profile of the injected electron bunches and the properties of the accelerated ones.

When a relativistic picosecond duration bunch passes within a few millimeters of an electro-optic crystal (like ZnTe and GaP), its transient electric field is equivalent to a half-cycle THz pulse impinging on the crystal. The temporal profile of this equivalent half-cycle THz pulse provides a faithful image of the longitudinal charge distribution inside the electron bunch if the electrons are

highly relativistic. The transient electric field induces birefringence in the electro-optic crystal. As the electric field propagates through the crystal, the birefringent properties of the crystal also propagate (see figure 6.2). This birefringence can be probed by a copropagating optical laser pulse being, in our case, the SPARC_LAB photocathode's laser, i.e., a titanium- sapphire (Ti:Sa) laser (100 fs pulse duration) with a wavelength of 800 nm.

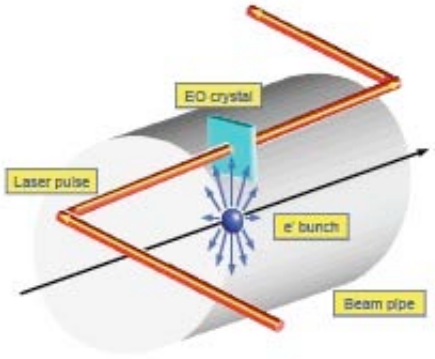

Figure 6.2: EOS working principle

The use of the same photocathode's laser enable us to have

- a simplified setup apparatus, since an independent laser system isn't necessary;
- always a synchronized laser with the electron beam;
- high laser's pulse energy available and low repetition rate (10 Hz); as a consequence, to image the laser beam, an intensified CCD (ICCD) isn't necessary and a commonly used CCD is sufficient.

The laser is sent from the SPARC_LAB Laser Room to the EOS Station through a transfer line (figure 6.3) consisting of 12 columns (height 2.2m), a laser pipe black anodized both internally and externally and two lenses (7.5m focuses) realizing a relay optics with 1:1 image ratio.

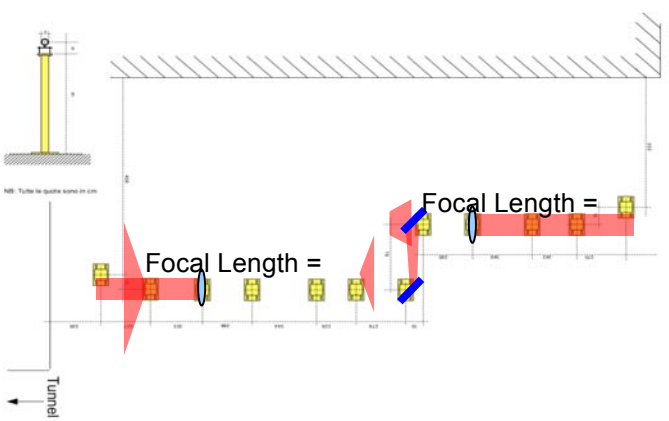

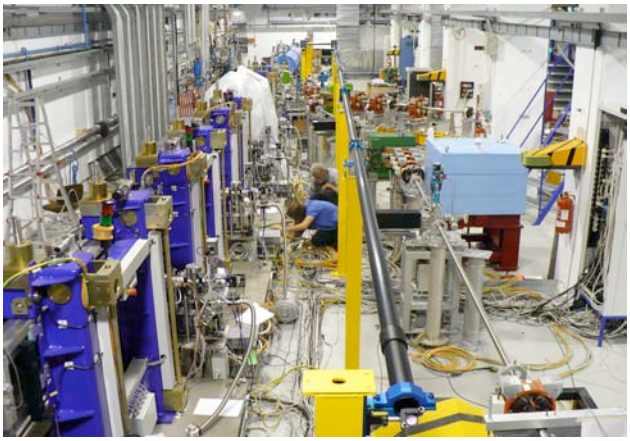

Figure 6.3: laser transfer line from the SPARC_LAB gun to the EOS Station

The EOS vacuum chamber has been realized and installed during 2012. The technical layout and the installation are reported in figure 6.4. The chamber is equipped with 3 axes: one for the electro-optic crystals and the beam targets (YAG, OTR) and two for the CCD Camera Autofocus.

Figure 6.5 shows the optical setup on the EOS station. Before passing in the nonlinear crystals, the laser is polarized and delayed (respect to the electron beam) through a motorized delay line. After the crystals it passes through another polarizer rotated by 90° respect to the first one. In such a way only the portion of the laser affected by the induced birefringence emerges from the second polarizer, and it can be measured by a CCD camera.

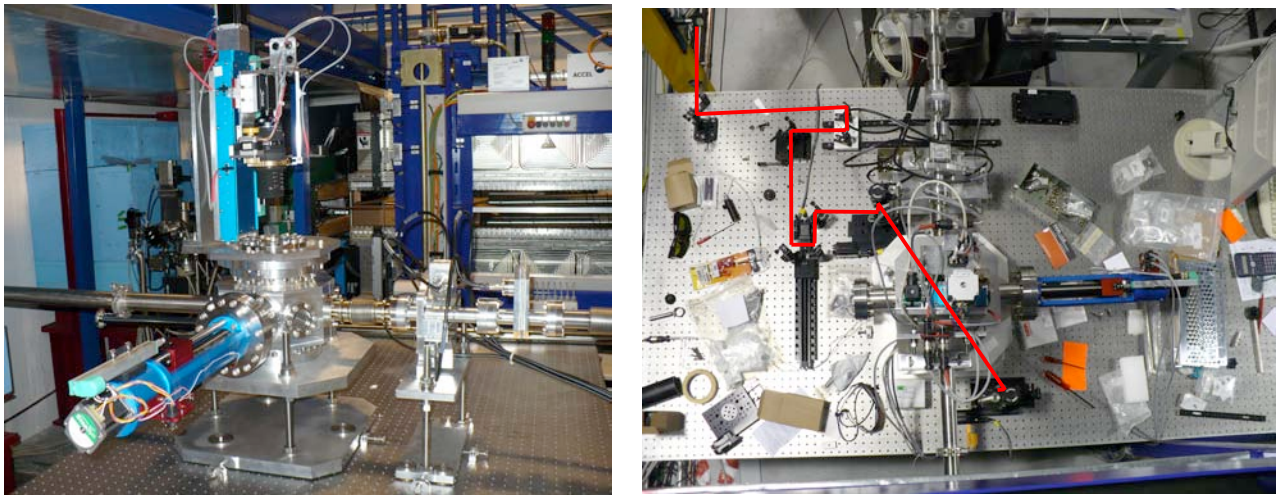

Figure 6.4: EOS chamber installed (left); EOS optical setup (right).

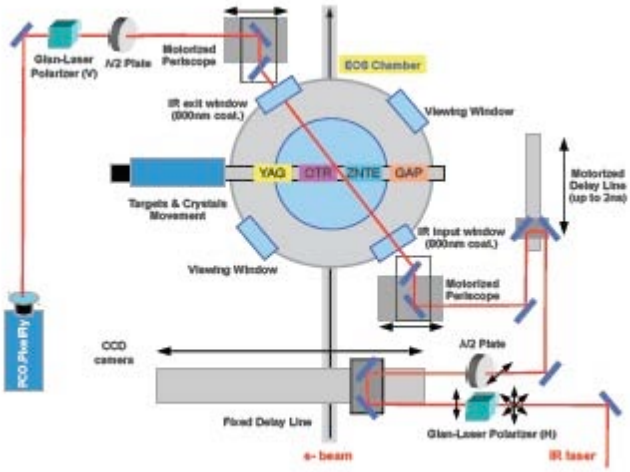

Figure 6.5: EOS optical detection scheme

During the last year the following goals have been achieved:

- realization, installation and test of the laser transfer line (32 meters long) from the SPARC_LAB photocathode to the EOS station;
- installation of the EOS Chamber with the nonlinear crystals (ZnTe and GaP);
- optical setup realized on the EOS station;

Now the experiment is ready to start with the measurements, that will be started from March.

References

[1] P. Muggli, Proc. of PAC 2009, Vancouver, Canada
[2] E. Chiadroni et al., Journal of Physics: Conference Series 357 (2012) 012034.
[3] A. Bacci et al, Proc. of FEL Conf. 2011, Shanghai, China.
[4] P. Tomassini, private communication.

7 TERASPARC experiment

P. Calvani (Resp., Ass.), M. Bellaveglia (Art. 23), M. Boscolo, M. Castellano (Ass.), M. Cestelli Guidi (Art. 23), E. Chiadroni, G. Di Pirro, M. Ferrario, G. Gatti, A. Nucara (Ass.), L. Palumbo (Ass.), R. Sorchetti (Tecn.), C. Vaccarezza

Participant institutions: other INFN sections (RM1, RM2, LNS, To)

The motivation for developing a linac-based THz source at SPARC stays in the ever growing interest of filling the so-called THz gap with high peak power radiation for both scientific and technological applications and longitudinal diagnostics issues. The THz radiation peak power expected at SPARC, and confirmed by measurements is in the order of 100 MW, corresponding energy per pulse is of the order of tens of μJ 1), 2) that is well above standard table top THz sources. Applications of this kind of source concern mainly time domain THz spectroscopy and frequency domain measurements on novel materials 3). Beyond these applications, coherent THz radiation is also used as longitudinal electron beam diagnostics to reconstruct the beam charge distribution 4). In addition, taking advantage from electron beam manipulation techniques, high power, narrow-band THz radiation can be also generated at SPARC 5, 6). This provides a unique chance to realize, with the SPARC THz source, THz-pump/THz-probe spectroscopy, a technique practically unexplored up to now.

The TERASPARC project, is a 3-years project, started in 2010, which aims at the generation, development and characterization of THz radiation produced by the SPARC photo-injector 7). TERASPARC is the result of a collaboration between LNF, INFN-Roma1, LNS, INFN-Torino, INFN-Roma2 and University of Roma Tor Vergata.

The source is Coherent Transition Radiation (CTR) from an aluminum coated silicon screen. CTR radiators are placed in the vacuum pipe, at 45° with respect to the electron beam direction (Figure 7.1), both at the end of the by-pass line and downstream from the third accelerating sections. The latter THz station holds also Diffraction Radiation (DR) screens with different slit apertures, i.e. 3 mm and 5 mm. Both TR and DR are extracted at 90° with respect to the beam axis through a z-cut quartz window and then collected by a 90° off-axis parabolic mirror. The parallel beam is then reflected down to a flat mirror at 45° which reflects radiation horizontally.

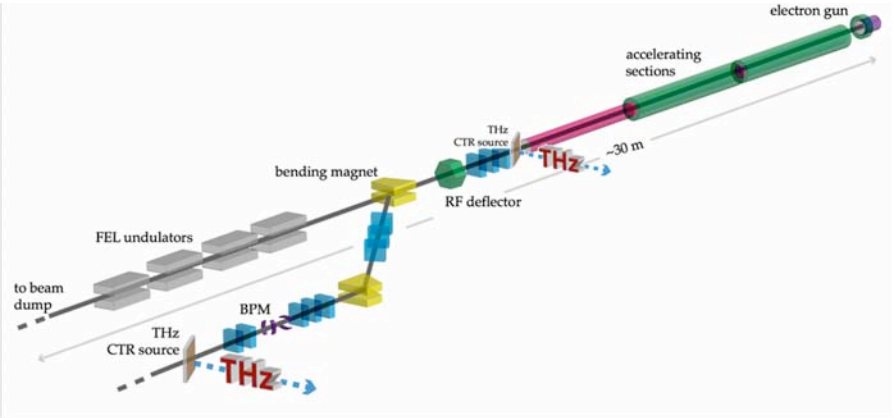

Figure 7.1: Layout of the SPARC accelerator, with the two THz sources placed at the linac exit and at the end of the by-pass line.

Two schemes are foreseen for the detection of both CTR and CDR spectra: one for interferometer measurements and one for integrated CTR/CDR measurements with the possibility of selecting custom band pass filters in the THz range 8).

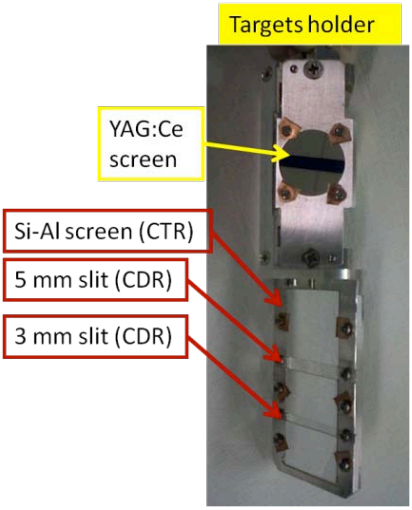

Figure 7.2: New targets holder, placed at the linac exit, for beam imaging (YAG:Ce screen) and both CTR and CDR generation.

Coherent radiation, both from the whole target (TR) and from part of it (DR), is emitted by both an ultra-short high-brightness electron beam and a longitudinally modulated one 6). In the former case high peak power broadband THz radiation is generated, while the latter, using a train of sub-ps electron bunches, is suitable for the production of narrow spectral bandwidth and tunable THz radiation. The technique used at SPARC to manipulate such electron beam relies on low energy RF compression, i.e. the velocity bunching technique 9) and on the use of properly shaped trains of UV laser pulses hitting the photo-cathode, i.e. laser comb beam schemes 10).

The activity in 2012 has been dedicated to the installation and commissioning of the new THz station downstream from the third accelerating section, hosting both CTR and CDR radiators.

The successful commissioning of the new THz station allowed us to compare the two sources under ultra-short single bunch operation, 300 pC bunch charge, 160 fs pulse duration, 120 MeV electron beam energy. The CTR energy per pulse, measured by means of a Golay cell detector in the spectral range between 150 GHz and 5 THz, is as high as 18 μJ (Figure 7.3), corresponding to electric and magnetic fields in the order of few MV/cm and sub-T, respectively. Figure 7.3 also shows the energy per pulse in case of CDR from both a 3 mm and 5 mm slit aperture, being in the order of few μJ.

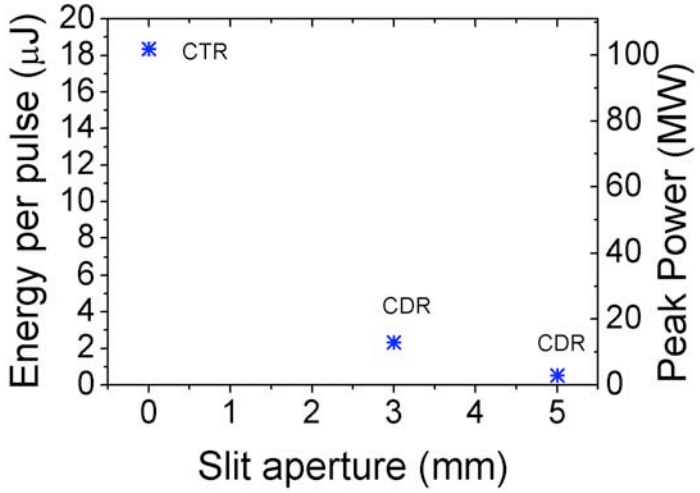

Figure 7.3: Measured CTR energy per pulse compared to that in case of CDR from both 3 mm and 5 mm slit aperture. Measurements are performed by means of a Golay cell detector in the spectral range from 150 GHz to 5 THz.

In addition, the CTR-based THz source has been used as diagnostic tool for the reconstruction of the electron beam longitudinal profile along the accelerator under different compression regimes. Indeed, the frequency analysis of the CTR autocorrelation function allows the reconstruction of the longitudinal temporal profile of the electron beam for different compression factors as obtained through the velocity bunching technique. An example of the retrieved results, for a 120 MeV and 300 pC electron beam, is shown in Figure 7.4, demonstrating the use of THz radiation also as a valid tool for the diagnosis of ultra-short electron bunches.

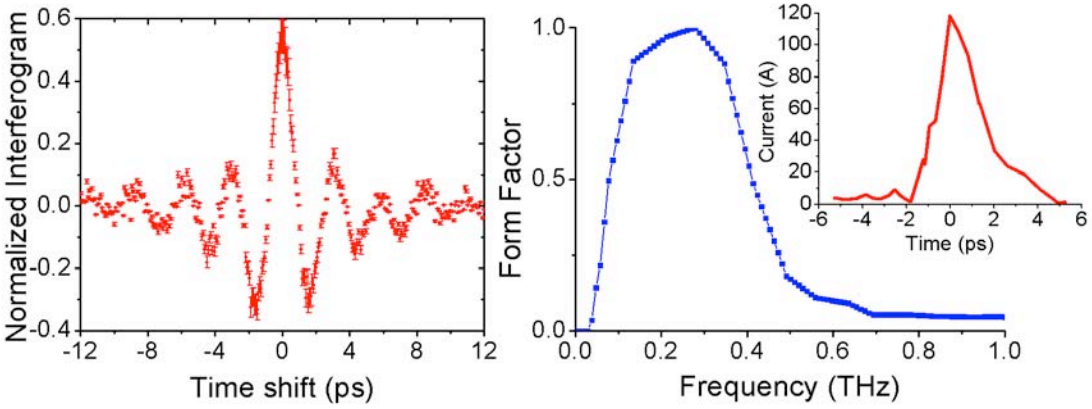

Figure 7.4: (Left) CTR autocorrelation function as measured through a Martin-Puplett interferometer. (Middle) Bunch form factor and, (right) the retrieved longitudinal bunch profile, providing a RMS bunch length of 1.4(0.10) ps.

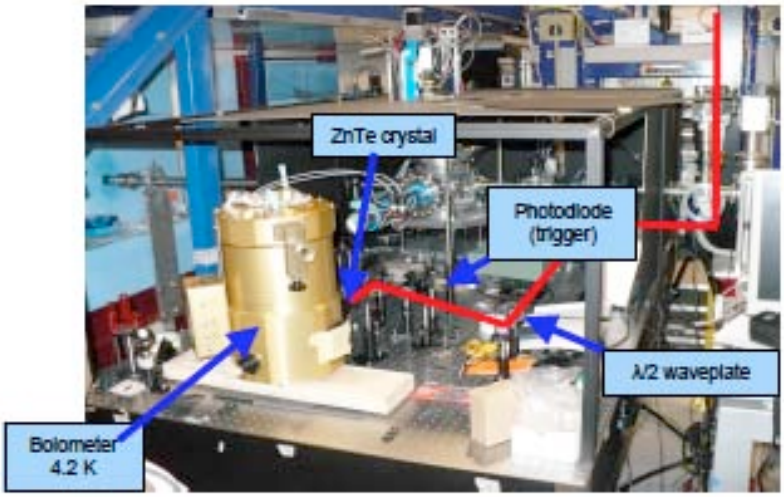

Figure 7.5: Experimental apparatus.

The latest achievement of 2012 regards the characterization of Electro-Optical (EO) crystals, being preparatory for the generation of THz radiation through Optical Rectifications and for the development of Electro-Optical Sampling (EOS) techniques, able to image the temporal profile of a transient THz pulse. Optical Rectification has been used in this preliminary experiment to characterize the ZnTe crystal axes orientation. Indeed, OR is a technique utilizing ultrafast laser pulses to generate broadband electromagnetic pulses in free space. The OR uses electro-optic crystals (like ZnTe) as a rectification medium and depending on the optical fluence the rectification is a second- order (difference frequency generation) or a higher-order nonlinear optical process. The THz amplitude depends on the laser's incident polarization angle. The experimental apparatus is shown in Figure 7.5. A titanium-sapphire (Ti:Sa) laser, 100 fs pulse duration, at a 800 nm wavelength, 52 μJ energy is split at the beginning into

a trigger beam (2μJ) sent to a photodiode and a pump beam (50 μJ). This one passes a half-wavelength wave-plate in order to change its polarization and then it is focalized with a lens on the 1 mm thick ZnTe crystal. Between the ZnTe crystal and the detector (a bolometer operating at 4.2 K) a Silicon screen is used to block the laser pulse, allowing only the so produced THz to be detected by the bolometer. The THz amplitude has been measured as function of the polarization angle of the laser as shown in Figure 7.6. This result allows to determine the [-1,1,0] axis of the crystal along which the laser's polarization needs to be directed to probe the birefringence change in future EOS experiments.

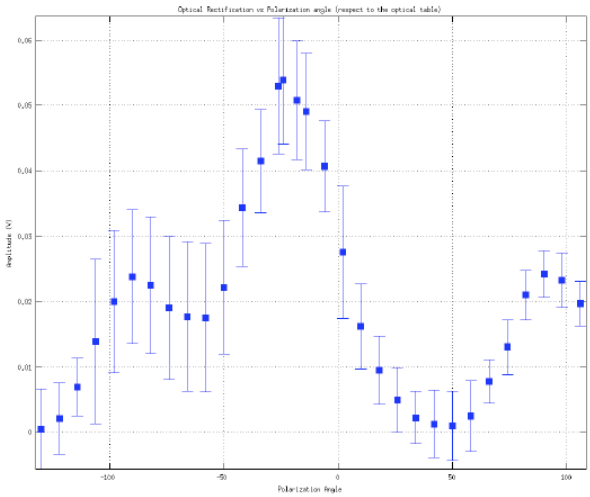

Figure 7.6: THz amplitude (in V) as function of the polarization angle (in deg).

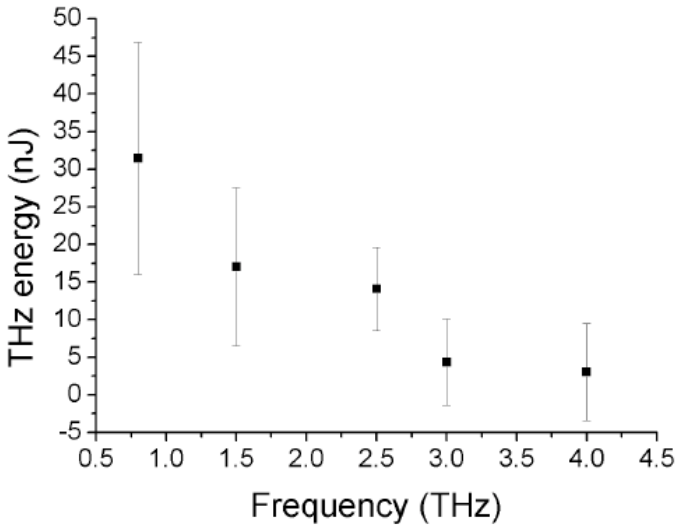

Figure 7.7: Measured THz radiation spectrum. The estimated energy takes into account the filters transmission (25%) and the bolometer responsivity (2.4*105 V/W).

Once defined the axis, the THz generation by optical rectification has been characterized as function of custom band-pass filters 8), the emission extending up to 4 THz. The corresponding THz energy has been retrieved assuming a 25% transmission for the band pass filters and a bolometer responsivity of 240 kV/W, see Fig 7.7

Publications in 2012

- E. Chiadroni, *The THz Beamlines at SPARC LAB*, Invited seminar at Karlsruhe Institut of Technology - ANKA (2012), Karlsruhe, Germany.
- E. Chiadroni, *Characterization of the THz radiation source at SPARC_LAB*, Oral contribution at the Workshop on Terahertz Sources for Time Resolved Studies of Matter, July 30-31, 2012, Argonne National Laboratory, Argonne, IL, USA.
- E. Chiadroni et al., J. Phys.: Conf. Ser. **357**, 012034 (2012).
- S. Lupi et al., J. Phys.: Conf. Ser. **359**, 012001 (2012).
- E. Chiadroni et al., J. Phys.: Conf. Ser. **359**, 012018 (2012).

Acknowledgment

Authors wish to thank colleagues collaborating from participant institutions:

- INFN Roma 1-La Sapienza: O. Limaj, S. Lupi
- University of Rome La Sapienza, SBAI: L. Palumbo, A. Mostacci
- INFN Roma 2-Tor Vergata: L. Catani, A. Cianchi, B. Marchetti, S. Tazzari
- INFN LNS: A. Rovelli
- INFN Torino: R. Gerbaldo, G. Ghigo, L. Gozzellino, E. Mezzetti, B. Minetti

References

[1] E. Chiadroni et al., Proc. of IPAC 2010, TUOARA03, Kyoto (2010).

[2] E. Chiadroni et al., "The SPARC linear accelerator based terahertz source", Appl. Phys. Lett. (in press) doi:10.1063/1.4794014.

[3] M.S. Sherwin et al., Opportunities in THz Science, Report of a DOE-NSF-NIH Workshop (2004).

[4] E. Chiadroni, "Bunch Length Characterization at the TTF VUV-FEL", TESLA-FEL 2006-09 (2006).

[5] A. Mostacci et al., Proc. of IPAC 2011, THYB01, San Sebastian (2011).

[6] E. Chiadroni et al., Rev. Sc. Inst. **84**, 022703 (2013).

[7] D. Alesini et al., Nucl. Instrum. and Meth. in Phys. Res. A 507, 345 (2003).

[8] N. I. Landy, 1-4244-1449-0/07/$25.00 c 2007 IEEE (2007); P. Carelli et al., unpublished (arXiv:0907.3620v2).

[9] M. Ferrario et al., Physical Review Letters 104, 054801 (2010).

[10] M. Ferrario et al., Nucl. Instrum. and Meth. in Phys. Res. A **637**, S43–S46 (2011).

8 POSSO experiment

S. Dabagov (Resp. Naz.), E. Chiadroni, G. Di Pirro, M. Ferrario, C. Vaccarezza

Recently we have started with a new project POSSO on studying the features of moderate-energies (0.1-1 GeV) electron beam channeling in various crystals [1]. The project aims in creating for a SPARC_LAB group both knowledge and experience for applying orientational behaviours of charged particles passage through the crystals to shape the beams (beam bending, collimation) as well as to generate a powerful x-ray and γ-radiation source (coherent bremsstrahlung, channeling radiation, parametric x-ray radiation) [2], see figure 8.1 and 8.2. One of the most interesting channeling-based application is a technique originated on its optimized combination with conventional methods for positron sources; electron channeling, namely channeling radiation by ultrarelativistic electrons (> 1 GeV) in crystals, is rather promising for getting high brilliant positron beams for the future e-/e+ colliders.

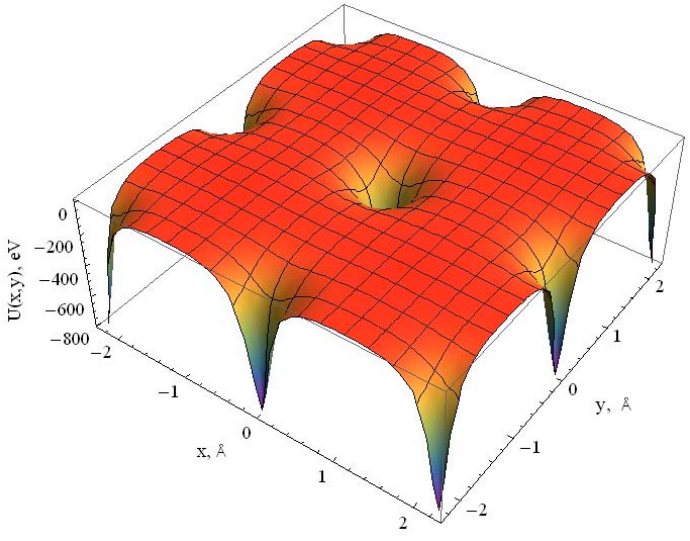

Figure 8.1: The averaged potential energy of electron interaction with W <100> crystallographic axis within the Doyle-Turner approximation. Due to extremely high gradiant of the potential well 102-103 GeV/m we can expect high flux of channeling radiation [2] .

Within the project we have performed theoretical studies that finalized in new computer codes for planar and axial channeling of relativistic electrons in various types of the crystals, detailed analysis of orientation features of electron scattering at axial channeling in very thin (submicron) monocrystals (studies on mirror reflection of the beam), detailed analysis of electron dechanneling and rechanneling at planar case based on solution of Fokker-Plank equations, getting the radiation power behind the crystals at the channeling orientations for various emittance parameters of the beam before the crystal, and electron beam simulations by the GEANT4-based codes for the optimization of experimental layout.

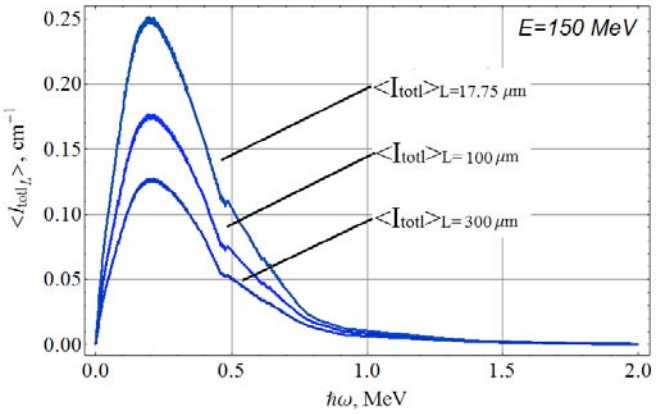

Figure 8.2: Total radiation yield of channeling radiation by single electron per unit of a Si (110) crystal length for 3 various crystal thicknesses. In final design the thickness should be optimized.

With the increase of electron energy the radiation loss due to the beam channeling becomes essential; for instance, for the electron energy change from 150 MeV to 200 MeV the radiation intensity in Si (110) increases two times, while for 800 MeV electrons the radiation flux becomes one order higher. Keeping in mind that the depth of a Si (110) potential well (~20 eV) is much less deeper than the one for a W <100> (~800 eV), we can expect extremely high channeling radiation flux in W to be emitted witin the cone of $1/\gamma \sim 10\text{-}3$ [2].

Additionally, together with the SPARC_LAB team we have evaluated various possible solutions for a new beam line dedicated to channeling studies, and, finally, have chosen the layout to be constructed as a continuation of the dogleg piece of the THz beamline.

References

[1] S.B. Dabagov, N.K. Zhevago, La Rivista del Nuovo Cimento 31 (9), 491 (2008).
[2] S.B. Dabagov et al. IJMPh A 22 (23) 4280 (2007).